Uncertainty of Measurement Error in Intelligent Electronic Devices

Po-Chen Chen[1], *Student Member, IEEE*, Yimai Dong[2], *Member, IEEE,* Vuk Malbasa[1], *Member, IEEE*, and Mladen Kezunovic[1], *Fellow, IEEE*

[1]Department of Electrical and Computer Engineering
Texas A&M University
College Station, TX 77843-3128, U.S.A.
pchen01@neo.tamu.edu, vmalbasa@tamu.edu, and
kezunov@ece.tamu.edu

[2]Electrocon International Inc.
Ann Arbor, MI 48103 USA
dongyimai@gmail.com

***Abstract*—This paper focuses on methodology to quantify uncertainty in measurements obtained from Intelligent Electronic Devices (IED). IEDs have emerged in distribution systems as a prevalent source of measurements in monitoring and protection, as well as for different kinds of applications beyond IED's primary purposes. These measurement devices are installed across a system, from substations down to the customer locations, and provide measurements of a wide array of quantities. We report how IED measurements respond to external disturbances, which may lead to possible accuracy impacts in various applications. The example used to illustrate the approach is highly accurate fault location in distribution systems based on voltage sag measurements.**

***Index Terms*—Fault location, Intelligent Electronic Device, measurement uncertainty, measurement units, smart grids.**

I. Introduction

The U.S. Department of Energy's initiative "GRID 2030" [1] has demonstrated a vision for the future modernization of power systems. Kezunovic *et al*. [2] have described the innovation process in the near future, which will require variations in the architecture and components of the current power grid, where Intelligent Electronic Devices (IEDs) are one of the essential components for monitoring and protection.

To date a wide variety of IEDs have become available and fielded. Some IEDs are performing waveform sampling in support of their primary applications (digital relays, digital fault recorder) [3]-[5], while others provide synchronized measurements in support of other applications (synchrophasor IEDs) [6]-[10]. Furthermore, some devices provide energy measurements and power quality indicators (smart meters and power quality meters) [11]-[14]. Fault location using IEDs plays a critical role in distribution systems for outage management and service restoration. For voltage sag based fault location [15]-[20] using data from variety of IEDs may in some cases have an advantage of detecting accurate fault location by matching the voltage measurements, while impedance-based methods may provide multiple ambiguous estimations [21]-[24].

As an example, voltage sag based fault location methods require accurate voltage measurements from the corresponding IEDs. Therefore, how the performance of IEDs varies with external disturbances becomes critical for accurate estimations [25], [26]. In this paper, we have characterized the uncertainty in measurements of a commercial IED product in order to validate its use for voltage sag based fault location. The device was tested in the Relay Testing Laboratory of Smart Grid Center, Texas Engineering Experiment Station (TEES). The tests were aimed at determining the parameters of measurement error under given fault scenario simulations.

II. Preparation for Testing

A. Requirements of IEDs used for Fault Location Measurements

As an important factor contributing to the accuracy of fault location, the characteristics of measurement error was determined by testing the IED product. Two characteristics of IED data were explored during the testing: quality (accuracy), and availability (how frequently the data is collected, the length of recording, etc.).

B. Test Signal Model

The test signal model describes the test waveforms. The steady-state signal model used in tests is

$$x(t) = \sum_{k=0} A_k \cos(2\pi k f_1 t + \varphi_k) + A_r \cdot r(t), \qquad (1)$$

where k is the order of harmonic, A_k is the amplitude of k^{th} harmonic, φ_k is the initial angle, f_1 is the fundamental frequency, A_r is the amplitude of random noise, and $r(t)$ is the

This material is based upon work supported by the Department of Energy under Award Number(s) DE-OE0000547. Funding for this effort comes from DOE through project titled "A real-time monitoring, control, and health management system to improve grid reliability and efficiency" awarded to ABB, Xcel Energy, and TEES.)

function generating random numbers from a normal distribution with μ=0 and σ =1.

C. Test Scenarios

The test scenarios shown in Table I include those for amplitude change, phase angle change, frequency change, and harmonic interference. The objective is to validate error in phasor amplitude and angle. Each scenario described in Table I has been replicated 10 times.

The reference conditions of Table I are $A_{k\_voltage} = \begin{cases} V_N, k = 1 \\ 0, k \neq 1 \end{cases}$, $A_{k\_current} = \begin{cases} I_N, k = 1 \\ 0, k \neq 1 \end{cases}$, $[\varphi_{1A}, \varphi_{1B}, \varphi_{1C}] = [0, -2\pi/3, 2\pi/3]$, A_r = 0, V_N = 100 V, and I_N = 1 A under 100% rated secondary value, constant phase, and nominal frequency.

D. Validating Quantities

In the steady state test scenarios the mean and variance of measurement error was calculated and we demonstrate the process using voltage amplitude. The error in test scenario *i* is defined as

$$error_{Vamp.i} = \frac{|V_{meas.i}| - |V_{ref.i}|}{|V_N|}, \quad (2)$$

where $|V_{meas.i}|$ is the measurement value from IED to secondary voltages, $|V_{ref.i}|$ is the reference voltage, and $|V_N|$ is the secondary-based voltage. Then the mean $Mean_{e\_Vamp}$ and the variance Var_{e_Vamp} of error can be computed as

$$Mean_{e\_Vamp} = \frac{\sum_{i=1}^{N_{Meas}} error_{Vamp.i}}{N_{Meas}}, \quad (3)$$

TABLE I. SENARIOS FOR STEADY-STATE TEST

Varying Quantity Name	Varying Quantity Variable	Varying Range	Step-Length
Line Voltage Amplitude	$\sqrt{3}A_{k\_voltage}$	0 – 120%	10%
Phase Current Amplitude	$A_{k\_current}$	0 – 500%	50%
Phase-to-Phase Voltage Angle Difference	$\varphi_{1A} - \varphi_{1B}$, $\varphi_{1B} - \varphi_{1C}$, and $\varphi_{1C} - \varphi_{1A}$	$\pi/6 - 2\pi/3$	$\pi/6$
Line Voltage Amplitude	$\sqrt{3}A_{k\_voltage}$	0 – 120%	10%
Phase-to-Phase Current Angle difference	$\varphi_{1A} - \varphi_{1B}$, $\varphi_{1B} - \varphi_{1C}$, and $\varphi_{1C} - \varphi_{1A}$	$\pi/6 - 2\pi/3$	$\pi/6$
Frequency	f_1	59 – 61 Hz	0.5 Hz
Harmonics Amplitude	A_k, k = 3, 5, 9	5% and 10%	5%

$$Var_{e\_Vamp} = \frac{\sum_{i=1}^{N_{Meas}} (error_{Vamp.i} - Mean_{e\_Vamp.i})^2}{N_{Meas}}, \quad (4)$$

where N_{Meas} is the number of measurement samples.

Errors in current amplitude measurements were calculated using the same formulations (2)-(4) by changing the voltage quantities to current quantities. This also applies to voltage and current angle measurements.

III. IMPLEMENTATION OF LAB TEST

A. Laboratory Setup

The hardware setup procedure is shown in Fig. 1. Test waveforms were generated and sent to analog signal amplifier via Input/Output (I/O) box and Digital/Analog (D/A) converter by Relay Assistant [27]; the Analog Signal Amplifier generates analog waveforms based on its input and sends them to the IED; amplitude measurements were read directly from IED's front panel screen; angle measurements were recorded by manually triggering the disturbance recording function, and retrieved from the disturbance reports.

The Techron 7780 Standard 3-phase Voltage/Current Multi-Amplifier System [28] from AE Techron was used as a signal amplifier set. After calibration, errors in output amplitudes ere within 0.1% rms, and errors in phase angle differences between outputs were within 0.5 degrees.

While performing laboratory experiments the amplitudes and reference quantities were obtained using the Fluke 8010A multimeter. When testing the angle, waveforms were captured by a Tektronix TDS 320 oscilloscope and the angle difference between two phases was calculated from time delays between zero-crossing points on two waveforms by

$$Angle_{ph1\_ph2} = 360 \cdot (T_{zero-cross\sin g, ph2} - T_{zero-cross\sin g, ph1}) \cdot f_0, \quad (4)$$

where $Angle_{ph1\_ph2}$ is the angle difference in degrees between phase 1 and phase 2 (1 and 2 being A, B or C), $T_{zero-cross\sin g, ph2} - T_{zero-cross\sin g, ph1}$ is the time delay between

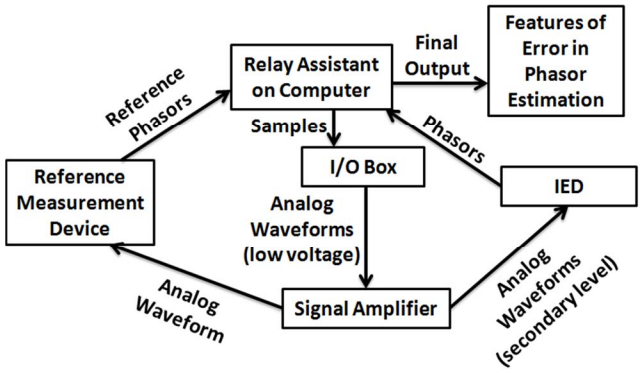

Figure 1: Hardware setup.

zero-crossing points on two waveforms, and f_0 is the fundamental frequency 60 Hz.

To analyze current waveforms the analog current signals were scaled down and converted to a voltage signal using a Jamb CT201T accurate current transformer, before connecting to the oscilloscope. To analyze voltage waveforms, 10:1 probes were applied to scale the voltage signals down before the oscilloscope sampled the signals.

B. Acquisition of Phasor Measurements from IED

Steady state signals lasting three seconds were sent to the IED and the reference measurement devices. Values were acquired in the middle of the signal generating process, when readings from IED and reference measurement devices were stable.

Values were read from the IED front panel screen. Angle measurements were retrieved from disturbance reports (example shown in Fig. 2). Recording of disturbances was triggered manually. In the meantime, the oscilloscope was triggered at the beginning of the test to produce reference measurement of angle difference between two phases.

C. Pre-processing of Data

All of the recorded data was converted to secondary quantities and compared to the readings from the reference measurement devices. For instance, when analyzing results from voltage amplitude tests, values from IED were first converted to secondary voltages using

$$V_{meas\_sec} = \frac{V_{meas\_prim} \cdot V_{N\_sec}}{V_{N\_prim}}, \quad (5)$$

where the quantities with subscript *sec* are secondary values, the quantities with subscript *prim* are primary values, and V_N means rated voltage on the primary or secondary side of the measurement transformer. Note that conversion of current measurements is similar to conversion of voltage measurements. Since line voltages (phase-to-phase voltage) were recorded, when calculating error using (2), $\sqrt{3}V_{N\_ph}$ was used as the rated line voltage.

When processing the results from angle tests, the angle differences between two phases were calculated from phase angles using the disturbance reports.

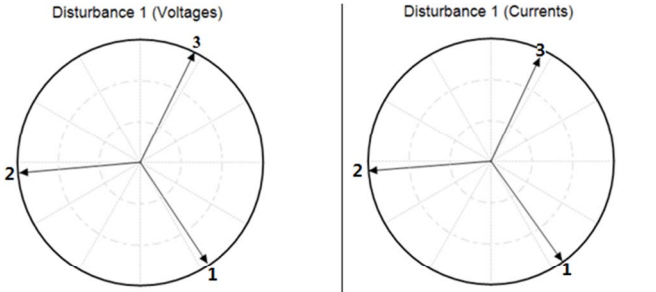

Figure 2: Phasor information from disturbance report.

IV. IED Setup and Test Procedure

The IED supports two measurement modes: RMS and DFT. The DFT algorithm filters out harmonics while the RMS method does not suppress harmonics. IED characterization includes harmonics and frequency tests which are affected by the measurement mode. The DFT mode was chosen in this study. Since the voltage sag based fault location algorithm requires a change in voltage amplitudes we used the DFT in order to filter out the harmonics.

A general procedure for performing the laboratory tests can be summarized as follows.

1. Calibrate amplifiers;
2. Generate test signals according to Table 1-3 using Relay Assistant;
3. Calibrate signals in Relay Assistant and send the calibrated signals to signal amplifier;
4. Record measurement values from IED and from reference measurement devices;
5. Move to next scenario and repeat the process.

V. Results and Analysis

Results from IED that characterized the mean quantities of the signal were shown in Fig. 3. Table II provides the data of V_{ab} in Fig. 3(a) as an example of test results (due to the space limits we cannot show all of them). Below is a summary of the observations.

1. Both voltage and current amplitude measurements produced very stable outputs during repeated tests, with very low variance. Offsets in both voltage and current amplitude measurements show a negative correlation with the amplitude of test signals. The errors show a linear pattern, suggesting that with proper settings of the amplitude correction factors, most of the error can be eliminated.
2. No obvious impacts of frequency and harmonics have been observed during tests of amplitude measurements.
3. Errors in angle measurements were not as stable as those in amplitude measurements, but the mean error in phase angle differences never exceeded ±5°; the largest absolute error detected was 8.6°.
4. No clear pattern in the angle difference errors, frequency or harmonics in the test waveforms was observed. The errors in angle differences may be related to the calculated phase angles, or the inception angles of the phasor calculation

TABLE II. Data of V_{AB} in Fig. 3(a): Errors in Line Voltage Amplitude Measurements to The Amplitude of Test Signal

Amplitude (per unit)	Mean [%]	Maximum [%]	Variance
0	1.9E-02	3.0E-02	9.1E-09
0.1	-1.8E-01	2.0E-01	6.6E-09
0.2	-2.8E-01	3.3E-01	2.3E-07
0.3	-4.8E-01	5.0E-01	6.9E-08
0.4	-5.7E-01	6.7E-01	1.1E-07
0.5	-6.3E-01	6.8E-01	7.0E-08
0.6	-9.0E-01	9.1E-01	9.0E-08
0.7	-1.1E+00	1.1E+00	1.5E-08
0.8	-1.2E+00	1.2E+00	2.0E-07
0.9	-1.4E+00	1.4E+00	0.0E+00
1	-1.6E+00	1.6E+00	2.4E-09
1.1	-1.8E+00	1.8E+00	5.4E-09
1.2	-1.9E+00	2.0E+00	1.9E-07

process when disturbance reports were generated.

Incidentally, the tests also reveal the constraint on using the measurements from the given IED in scenarios where the fault is cleared very quickly [29], [30]. The reporting mechanism of the device is designed such that a new measurement is reported when the accumulation of change over time exceeds a threshold. Therefore, the shortest fault duration for a during-fault measurement to be reported is 0.4 seconds under the most favorable settings and the most severe fault condition (voltage at measurement point drops to zero). Faults lasting less than 0.4 seconds would be interpreted as transients by the IED and the during-fault phasor measurements would be reported. In cases where faults are cleared by protective devices in less than a cycle (sub-cycle fault), employing fast and accurate phasor extraction techniques is necessary [20].

VI. CONCLUSIONS

This paper makes several contributions:

- A commercial IED product has been tested extensively in the lab to determine the parameters of measurement errors for fault scenario simulations.
- The impact of disturbances on the amplitude and angle of voltage and current measurements of IED was presented. The results demonstrate the observations of two different dimensions (as mentioned in Section II-A). The quality was sufficiently precise. The availability depends on how big the changes in amplitudes are and how long the during-fault period is.

ACKNOWLEDGMENTS

The authors gratefully acknowledge Dr. J. Stoupis, Dr. M. Mousavi, Dr. N. Kang, and Dr. X. Feng from the ABB Group for their feedback and valuable advice.

REFERENCES:

[1] GRID 2030, "A national vision for electricity's second 100 years."

[2] M. Kezunovic, V. Vittal, S. Meliopoulos, and T. Mount, "The Big Picture: Smart Research for Large-Scale Integrated Smart Grid Solutions," *IEEE Power and Energy Magazine*, vol. 10, no. 4, pp. 22 – 34, Jul. 2012.

[3] S. M. Brahma, P. L. De Leon, and R. G. Kavasseri, "Investigating the Option of Removing the Antialiasing Filter From Digital Relays," *IEEE Trans. Power Del.*, vol. 24, no. 4, pp. 1864-1868, Oct. 2009.

[4] P. M. Anderson, *Power System Protection*, Wiley-IEEE Press, 1999.

[5] Distributed Digital Fault Recorder, Digital Energy, General Electric.

[6] M. Kezunovic and B. Perunicic, "Automated Transmission Line Fault Analysis Using Synchronized Sampling at Two Ends," *IEEE Trans. Power Syst.,* Vol. 11, No. 1, Feb. 1996.

[7] W. Premerlani, B. Kasztenny, and M. Adamiak, "Development and Implementation of a Synchrophasor Estimator Capable of Measurements Under Dynamic Conditions," *IEEE Trans. Power Del.*, vol. 23, no. 1, pp. 109-123, Jan. 2008.

[8] J. De La Ree, V. Centeno, J. S. Thorp, and A. G. Phadke, "Synchronized Phasor Measurement Applications in Power Systems," *IEEE Trans. Smart Grid*, vol. 1, no. 1, pp. 20-27, Jun. 2010.

[9] K. E. Martin, D. Hamai, M. G. Adamiak, S. Anderson; M. Begovic, G. Benmouyal, G. Brunello, J. Burger, J. Y. Cai, B. Dickerson, V. Gharpure, B. Kennedy, D. Karlsson, A. G. Phadke, J. Salj, V. Skendzic, J. Sperr, Y. Song, C. Huntley, B. Kasztenny, and E. Price, "Exploring the IEEE Standard C37.118–2005 Synchrophasors for Power Systems," *IEEE Trans. Power Del.*, vol. 23, no. 4, pp. 1805-1811, Oct. 2008.

[10] C. Zheng, V. Malbasa, and M. Kezunovic, "Regression tree for stability margin prediction using synchrophasor measurements," *IEEE Trans. Power Syst.*, vol. 28, no. 2, pp. 1978-1987, May 2013.

[11] H. S. Cho, T. Yamazaki, and Minsoo H, "Determining location of appliances from multi-hop tree structures of power strip type smart meters," *IEEE Trans. Consum. Electron.*, vol. 15, no. 4, pp. 1169-1174, Oct. 2000.

[12] K. Koziy, B. Gou, and J. Aslakson, "A Low-Cost Power-Quality Meter With Series Arc-Fault Detection Capability for Smart Grid," *IEEE Trans. Power Del.*, vol. 28, no. 3, pp. 1584-1591, Apr. 2013.

[13] J. Momoh, *Smart Grid: Fundamentals of Design and Analysis*, John Wiley & Sons, Mar. 2012

[14] L. Cristaldi, A. Ferrero, and S. Salicone, "A distributed system for electric power quality measurement," *IEEE Trans. Instrum. Meas.*, vol. 51, no. 4, pp.776-781, Aug. 2002.

[15] R. A. F. Pereira, L. G. W. Silva, M. Kezunovic, and J. R. S. Mantovani, "Improved fault location on distribution feeders based on matching during-fault voltage sags," *IEEE Trans. Power Del.*, vol. 24, no. 2, pp. 852–862, Apr. 2009.

[16] S. Lotfifard, M. Kezunovic, and M. J. Mousavi, "A Systematic Approach for Ranking Distribution Systems Fault Location Algorithms and Eliminating False Estimates," *IEEE Trans. Power Del.*, vol. 28, no. 1, pp. 285-293, Jan. 2013.

[17] Y. Dong, C. Zheng, and M. Kezunovic, "Enhancing Accuracy While Reducing Computation Complexity for Voltage sag based Distribution Fault Location," *IEEE Trans. Power Del.*, vol. 28, no. 2, pp. 1202–1212, Apr. 2013.

[18] P.-C. Chen, V. Malbasa, M. Kezunovic, and Y. Dong, "Sensitivity of Voltage Sag Based Fault Location in Distribution Network to Sub-Cycle Faults," submitted to *IEEE/PES General Meeting*, 2014.

[19] P.-C. Chen, V. Malbasa, and M. Kezunovic, "Sensitivity Analysis of Voltage Sag Based Fault Location Algorithm," submitted to Power Systems Computation Conference (PSCC), Wroclaw, Poland, 2014.

[20] P.-C. Chen, V. Malbasa, and M. Kezunovic, "Locating Sub-Cycle Faults in Distribution Network Applying Half-Cycle DFT Method," accepted for publication in *IEEE/PES Transmission and Distribution Conference and Exposition (T&D)*, 2014.

[21] A. A. Girgis, C. M. Fallon, and D. L. Lubkeman, "A fault location technique for rural distribution feeders," *IEEE Trans. Ind. Appl.*, vol. 29, no. 6, pp. 1170–1175, Dec. 1993.

[22] L. Yuan, "Generalized fault-location methods for overhead electric distribution systems," *IEEE Trans. Power Del.*, vol. 26, no. 1, pp. 53–64, Jan. 2011.

[23] S. Das, N. Karnik, and S. Santoso, "Distribution fault-locating algorithms using current only," *IEEE Trans. Power Del.*, vol. 27, no. 3, pp. 1144–1153, Jul. 2012.

[24] R. H. Salim, M. Resener, A. D. Filomena, K. R. Caino de Oliveira, and A. S. Bretas, "Extended fault-location formulation for power distribution systems," *IEEE Trans. Power Del.*, vol. 24, no. 2, pp. 508–516, Apr. 2009.

[25] M. Kezunovic, "Smart Fault Location for Smart Grids," *IEEE Trans. on Smart Grid*, vol. 2, No. 1, pp 11-22, Mar. 2011.

[26] M. Kezunovic, L. Xie, and S. Grijalva, "The role of big data in improving power system operation and protection," *Bulk Power System Dynamics and Control - IX Optimization, Security and Control of the Emerging Power Grid (IREP)*, pp. 1-9, Aug. 2013.

[27] "Relay Assistant for Transient Relay Testing", Megger and Test Laboratories International (TLI) product datasheet. [Online]. Available: http://www.tequipment.net/pdf/Megger/RelayAssistantDataSheet.pdf

[28] "7700 Series Power Supply Amplifiers Technical Manual", technical manual, AE Techron, January 1997.

[29] C. J. Kim. and T. O. Bialek, "Sub-cycle ground fault location — Formulation and preliminary results," *IEEE/PES Power Systems Conference and Exposition (PSCE)*, pp. 1-8, Mar. 2011.

[30] R. Moghe, M. J. Mousavi, J. Stoupis, and J. McGowan, "Field investigation and analysis of incipient faults leading to a catastrophic failure in an underground distribution feeder," *IEEE/PES Power Systems Conference and Exposition (PSCE)*, pp. 1-6, Mar. 2009.

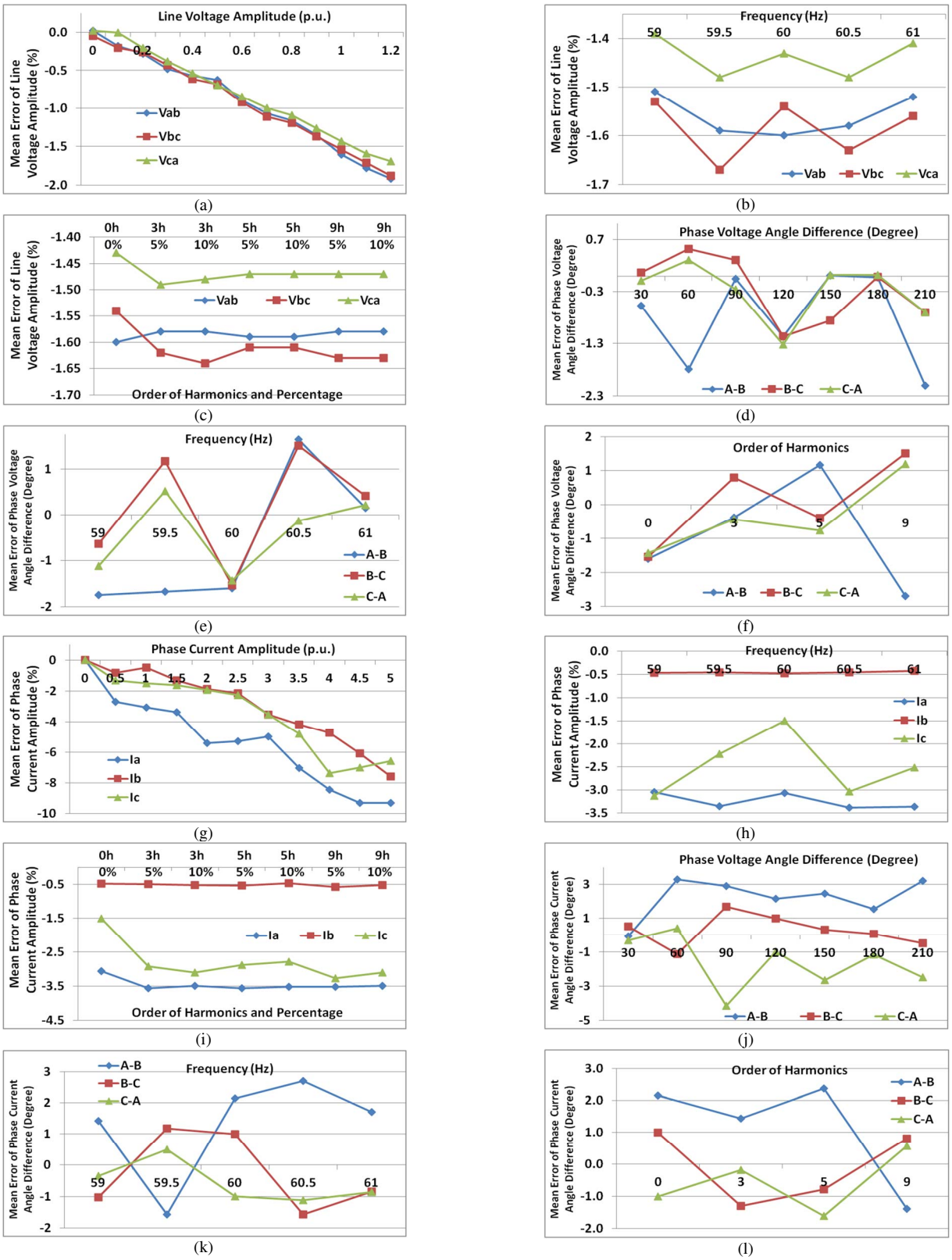

Figure 3: All the quantities are referred to the test signal, and the quantities of y-axis are referred to mean errors in the sub-figure descriptions; (a) line voltage amplitude vs. line voltage amplitude; (b) line voltage amplitude vs. frequency; (c) line voltage amplitude vs. harmonic level; (d) phase voltage angle difference vs. phase voltage angle difference; (e) phase voltage angle differences vs. frequency; (f) phase voltage angle difference vs. harmonic level; (g) phase current amplitude vs. phase current amplitude; (h) phase current amplitude vs. frequency; (i) phase current amplitude vs. harmonic level; (j) phase current angle difference vs. phase current angle difference; (k) phase current angle difference vs. frequency; (l) phase current angle difference vs. harmonic level.